# Collision Dynamics of Two $^{238}$U Atomic Nuclei

Cédric Golabek
*GANIL (IN2P3/CNRS - DSM/CEA), BP 55027, F-14076 Caen Cedex 5, France*

Cédric Simenel
*CEA, Centre de Saclay, IRFU/Service de Physique Nucléaire, F-91191 Gif-sur-Yvette, France*
(Received 20 April 2009; revised manuscript received 19 May 2009; published 24 July 2009)

Collisions of actinide nuclei form, during very short times of few $10^{-21}$ s, the heaviest ensembles of interacting nucleons available on Earth. Such collisions have been proposed as an alternative way to produce heavy and superheavy elements. They are also used to produce superstrong electric fields by the huge number of interacting protons to test spontaneous positron-electron ($e^+e^-$) pair emission predicted by the quantum electrodynamics theory. The time-dependent Hartree-Fock theory is used to study collision dynamics of two $^{238}$U atomic nuclei. In particular, the role of nuclear deformation on collision time and on reaction mechanisms such as nucleon transfer is emphasized. The highest collision times ($\sim 4 \times 10^{-21}$ s at 1200 MeV) should allow experimental signature of spontaneous $e^+e^-$ emission in case of bare uranium ions. Surprisingly, we also observe ternary fission due to purely dynamical effects.

DOI: 10.1103/PhysRevLett.103.042701 PACS numbers: 25.70.−z, 21.60.Jz, 31.30.J−

The study of nuclei with more than 100 protons is strongly motivated by the desire to understand quantum mechanics at the scale of few femtometers as there existence relies only on quantum shell effects. Indeed, in a purely classical world, i.e., without shell structure, transfermium nuclei would undergo fission within about $10^{-20}$ s due to the strong Coulomb repulsion between their protons. Superheavy elements (SHEs) are searched to localize the next island of stability in the top of the nuclear chart [1–5]. They also provide a crucial test to modern atomic models as their chemical properties might deviate from their homologue elements in the periodic table due to strong relativistic effects on the valence electron shells [6]. Recently, SHEs have been synthesized through ''cold'' fusion reactions based on closed shell target nuclei [1,2] and with ''hot'' fusion reactions involving actinide targets [3,4]. However, the decay chains of nuclei formed by hot fusion do not populate presently known nuclei and a ''blank spot'' exists in the nuclear chart around $Z = 105$ and $N = 160$. Modern experimental techniques might be used to explore this region with multinucleon transfer between actinides [7], and, thus, deserve theoretical investigations.

Our study also deals with the possibility to produce $e^+e^-$ spontaneous emission in such collisions [8–10]. No experimental evidence of this process has been obtained so far [11]. One limiting factor is the Pauli blocking effect due to an occupation of the final state by surrounding electrons. However, future facilities like the GSI-FAIR project should be able to get rid of this limitation using bare uranium-uranium merged-beam collisions. Reliable predictions of collision times are needed to optimize the energy of the reaction. Recent calculations based on the time-dependent Dirac equation [10] show that two bare $^{238}$U need to stick together during at least $2.10^{-21}$ s to allow observation of spontaneous positron emission. Although no pocket exists in the nucleus-nucleus potential of this system [12,13], nuclear attraction reduces Coulomb repulsion and dissipation mechanisms such as evolution of nuclear shapes may delay the separation of the system [7]. Recently, delay times in this reaction was searched analyzing kinetic energy loss and mass transfer [14]. Theoretically, the complexity of reaction mechanisms and the high number of degrees of freedom to be included motivate the use of microscopic approaches. First, dynamical microscopic calculations of $^{238}$U + $^{238}$U have been performed recently thanks to the Quantum Molecular Dynamics (QMD) model [15]. Though a major step forward has been done in terms of predictive power with these calculations, improvements are still mandatory. In particular, the strong ground state deformation of $^{238}$U is not included, and nucleon wave functions are constrained to be Gaussian wave packets. In addition, the Pauli principle is only approximately treated in QMD.

Here, we overcome these limitations by authorizing all spatial forms of the nucleon wave functions. The time-dependent Hartree-Fock (TDHF) theory [16] is used with a Skyrme energy density functional (EDF) modeling nuclear interactions between nucleons [17]. The EDF is the only phenomenological ingredient, as it has been adjusted on nuclear structure properties [18]. The main approximation of this theory is to constrain the many-body wave function to be an antisymmetrized independent particles state at any time. It ensures an exact treatment of the Pauli principle during time evolution. Though TDHF does not include two-body collision term, it is expected to treat correctly one-body dissipation which is known to drive low-energy reaction mechanisms as Pauli blocking prevents nucleon-

 

nucleon collisions. Inclusion of pairing correlations have been done only recently with a full Skyrme EDF within the time-dependent Hartree-Fock-Bogolyubov theory [19]. However, realistic applications to heavy ions collisions are not yet achieved and are beyond the scope of this work. At initial time, the nuclei are in their Hartree-Fock ground state allowing for a fully consistent treatment of nuclear structure and dynamics.

The TDHF equation can be written as $i\hbar\frac{\partial}{\partial t}\rho = [h[\rho], \rho]$ where $\rho$ is the one-body density matrix associated to the total independent particles state with elements $\rho(\mathbf{r}sq, \mathbf{r}'s'q') = \sum_{i=1}^{A_1+A_2} \varphi_i(\mathbf{r}sq)\varphi_i^*(\mathbf{r}'s'q')$ where $A_1$ and $A_2$ are the number of nucleons in the nuclei. The sum runs over all occupied single particle wave functions $\varphi_i$ and $\mathbf{r}$, $s$, and $q$ denote the nucleon position, spin, and isospin, respectively. The single particle Hamiltonian $h[\rho]$ is related to the Skyrme EDF, noted $E[\rho]$, which depends on local densities [20] by $h[\rho](\mathbf{r}sq, \mathbf{r}'s'q') = \frac{\delta E[\rho]}{\delta\rho(\mathbf{r}'s'q',\mathbf{r}sq)}$.

First TDHF calculations were restricted to one dimension [21]. Recent increase of computational power allowed realistic TDHF calculations in 3 dimensions with modern Skyrme functionals including spin-orbit term [22–24]. Here, the TDHF equation is solved iteratively in time on a spatial grid with a plane of symmetry (the collision plane) using the TDHF3D code with the SLy4$d$ parameterization of the Skyrme EDF [22]. The lattice spacing is $\Delta x = 0.8$ fm, and the time step is $\Delta t = 1.5 \times 10^{-24}$ s (see Ref. [25] for more details). This code has been extensively used to study heavy ions fusion [13,26–29]. In particular, it reproduces average fusion barriers very well with no input from reaction mechanisms [27,28]. Recent calculations also indicate that TDHF can be used to study the fusion hindrance observed in heavy quasisymmetric systems [13] which encourages applications to heavier systems.

The $^{238}$U nucleus exhibits a prolate deformation with a symmetry axis in its ground state. The effect of this deformation on collision is investigated in four configurations ($xx$, $yx$, $yy$, and $yz$) associated to different initial orientations. The letters $x$, $y$, and $z$ denote the symmetry axis of the nuclei which collide along the $x$ axis (see Fig. 1). We focus on central collisions as they lead to the most dissipative reactions with the longest collision times.

First, we analyze the fragments produced in exit channels. Strictly speaking, they are *primary* fragments as they might decay by statistical fission. This decay is not studied here as it occurs on a much longer time scale than the collision itself. The importance of initial orientation on reaction mechanism is clearly seen in Fig. 1. Snapshots of isodensities are plotted at $E_{\text{c.m.}} = 900$ MeV. The $yy$ configuration gives two symmetric fragments because, in this case, the $x = 0$ plane is a plane of symmetry, although nucleon transfer is still possible thanks to particle number fluctuations in the fragments. Nucleon transfer is expected to be stronger in the $yx$ configuration because, in addition to fluctuations, no spatial symmetry prevents from an average flux of nucleons. Indeed, integration of densities in each reactant after the $yx$ collision indicates an average transfer of ~6 protons and ~11 neutrons from the tip of the aligned nucleus to the side of the other. The $yx$ configuration is then expected to favor the formation of nuclei heavier than $^{238}$U.

The role of collision energy is shown in Fig. 2(a). Two regimes can clearly be identified. At $E_{\text{c.m.}} \leq 1000$ MeV, standard transfer dominates and nuclei up to $^{253}$Cf are produced from the average flux of nucleons. In this energy regime, the heavy fragment may survive to fission but is not expected to reach the SHE region. This is consistent with experimental observations [30]. Here, single particle wave functions are transferred through the neck between the fragments with a smooth change of their shapes. In particular, the particle density in the neck increases with energy but is always lower than the saturation density $\rho_0 = 0.16$ fm$^{-3}$. This value is reached only at $E_{\text{c.m.}} \sim 1000$ MeV. At higher energies, however, the contact area gets more dense, and saturation density is overcome in the neck. This modifies dynamically the breaking point of the giant system, and the left fragment gains much more nucleons than expected in standard transfer. Superheavy fragments up to $Z \sim 130$ and $N \sim 205$ could be produced at $E_{\text{c.m.}} \sim 1500$ MeV. However, at these energies, the heavy fragment is expected to have a very high temperature and to decay into fission. Note that, for such violent collisions, nucleon-nucleon collisions might play a role on top of the mean-field evolution and extensions of TDHF including collision term should be considered to check these predictions [31–33].

Figure 1 also shows that, in the $xx$ configuration, the giant system breaks in three fragments. This was a surprise as a static macroscopic approach predicted this phenomenon to be strongly hindered as compared to binary fission [34]. Here, integration of densities indicates a $^{16}$C-like fragment. Why does the system decide to form a third

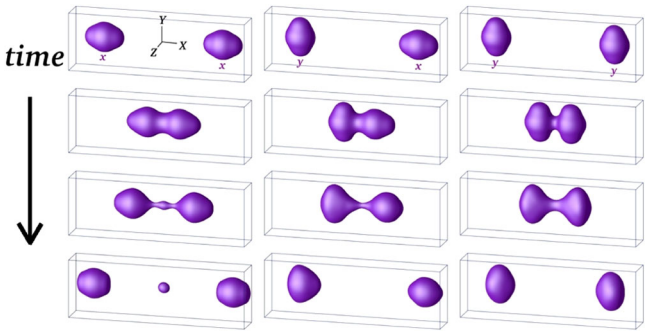


FIG. 1 (color online). Isodensities at half the saturation density, i.e., $\rho_0/2 = 0.08$ fm$^{-3}$, in $^{238}$U + $^{238}$U central collision at a center of mass energy $E_{\text{c.m.}} = 900$ MeV. Evolutions associated to the three initial configurations $xx$, $yx$, and $yy$ are plotted in the left, middle, and right column, respectively. Snapshots are given at times $t = 0$, 15, 27, and $42 \times 10^{-22}$ s from top to bottom.

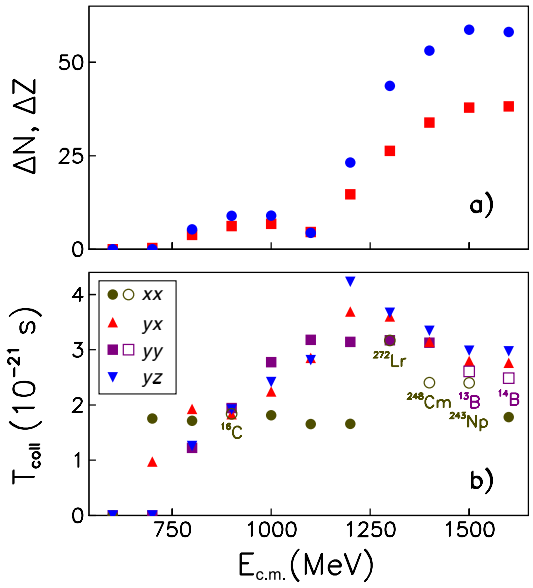


FIG. 2 (color online). (a) Number of transferred protons (squares) and neutrons (circles) in the $yx$ configuration and (b) collision times for each orientation as function of center of mass energy. Empty symbols indicate that three fragments are produced in the exit channel. In this case, the closest nucleus to the middle fragment is given.

fragment instead of breaking at the neck? The answer is given by a close look at its internal density. Figure 3 shows a snapshot of the density at closest approach. The density reaches 0.166 fm$^{-3}$ in the neck, exceeding $\rho_0$. This places the system in the ternary fission valley of the potential energy surface. To many charges are present in the center and the Coulomb energy is not efficient to compensate for the surface energy increase which induces the formation of two necks [34]. The same phenomenon is observed in the $yy$ configuration at $E_{c.m.} = 1500$ and 1600 MeV. Here, the middle fragment corresponds to a neutron rich boron isotope [see Fig. 2(b)]. This occurs at higher energy than in the $xx$ case because a closer distance is needed to overcome $\rho_0$ in the neck. (To reach closer distances, the nuclei need more energy as the Coulomb repulsion get stronger.) Note that overcoming saturation density is not a sufficient condition to produce three fragments as, e.g., such an exit channel is not observed in the $yz$ configuration. A third (heavy) fragment is also produced at high energy in the $xx$ configuration [see Fig. 2(b)]. In this case, however, the dynamics is driven by strong density fluctuations similar to the high-energy regime in the $yx$ configuration [see Fig. 2(a) and above discussion on transfer].

We finally investigate the collision time between nuclei. Here, it is defined as the time during which the neck density exceeds $\rho_0/10$. Figure 2(b) shows the evolution of collision time $T_{coll}$. At $E_{c.m.} \leq 900$ MeV, three distinct behaviors between the $xx$, $yx$, and $yy/yz$ configurations are seen. In particular, the last need more energy to get into contact as the energy threshold above which nuclear interaction plays a significant role is higher for such compact configurations.

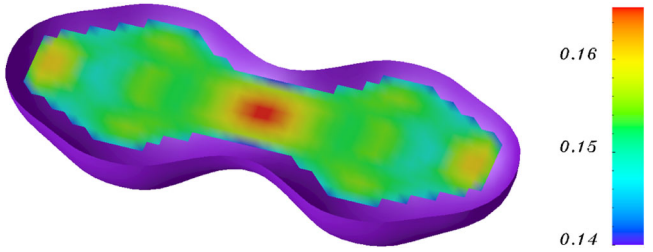


FIG. 3 (color online). Nucleon density (in fm$^{-3}$) in the collision plane is plotted when the density in the neck reaches its maximum in the $xx$ configuration at $E_{c.m.} = 900$ MeV. The half cut surface is an isodensity at $\rho_0/2$.

At all energies, the $yx$, $yy$, and $yz$ orientations exhibit roughly the same behavior, i.e., a rise and fall of $T_{coll}$ with a maximum of $3 - 4 \times 10^{-21}$ s at $E_{c.m.} \sim 1200$ MeV. This position of the maximum is in agreement with Ref. [15]. Dynamical evolution of nuclear shapes in these three configurations and a strong transfer in the $yx$ one are responsible for these rather long collision times as compared to scattering with frozen shapes of the reactants [7]. The $xx$ configuration, however, behaves differently. $T_{coll}$ exhibits a plateau which does not exceed $2 \times 10^{-21}$ s except when a third heavy fragment is formed. This overall reduction of $T_{coll}$ in the $xx$ case is attributed to the strong overlap of the tips, producing a density in the neck higher than $\rho_0$ (see Fig. 3). The fact that nuclear matter is difficult to compress translates into a strong repulsive force between the fragments which decreases their contact time. This phenomenon is also responsible for the fall of collision times in the other configurations, though higher energies are needed to strongly overlap.

To conclude, this fully microscopic quantum investigation of the $^{238}$U + $^{238}$U reaction exhibits a rich phenomenology strongly influenced by the shape of the nuclei. Three main conclusions can be drawn. (i) The giant system formed in bare uranium-uranium central collisions is expected to survive enough time to allow experimental observation of spontaneous positron emission, but only for some initial orientations (which reduces slightly the cross section of the process) and with an energy $E_{c.m.} \geq 1000$ MeV. (ii) Heavy fragments produced at low energy might survive fission, but the center of their charge distribution does not reach the transfermium region. We expect more systematic studies of other actinide collisions in a near future to look for optimized channels for transfermium and SHE productions, making use, for instance, of the "inverse quasifission" process [7]. (iii) Experimental observation of carbonlike fragments at $E_{c.m.} = 900$ MeV would sign ternary fission. We encourage experimental and theoretical investigations of this mechanism as it is an excellent probe to test the physical ingredients of this microscopic approach. In particular, how is it affected by

the different terms of the energy density functional and what is the effect of pairing are open questions.

We thank P. Bonche for providing his code. We are also grateful to B. Avez, D. Boilley, R. Dayras, W. Greiner, S. Heinz, and A. Villari for discussions and a careful reading of the Letter. The calculations have been performed in the Centre de Calcul Recherche et Technologie of the Commissariat à l'Énergie Atomique.

[1] S. Hofmann and G. Münzenberg, Rev. Mod. Phys. **72**, 733 (2000).
[2] K. Morita *et al.*, J. Phys. Soc. Jpn. **76**, 045001 (2007).
[3] Yu. Ts. Oganessian *et al.*, Phys. Rev. C **74**, 044602 (2006).
[4] S. Hofmann *et al.*, Eur. Phys. J. A **32**, 251 (2007).
[5] M. Morjean *et al.*, Phys. Rev. Lett. **101**, 072701 (2008).
[6] R. Eichler *et al.*, Nature (London) **447**, 72 (2007).
[7] V. I. Zagrebaev, Yu. Ts. Oganessian, M. G. Itkis, and W. Greiner, Phys. Rev. C **73**, 031602(R) (2006).
[8] *Quantum Electrodynamics of Strong Fields*, edited by W. Greiner (Plenum, New York, 1983).
[9] J. Reinhardt, B. Müller, and W. Greiner, Phys. Rev. A **24**, 103 (1981).
[10] E. Ackad and M. Horbatsch, Phys. Rev. A **78**, 062711 (2008).
[11] I. Ahmad *et al.*, Phys. Rev. C **60**, 064601 (1999).
[12] J. F. Berger, J. D. Anderson, P. Bonche, and M. S. Weiss, Phys. Rev. C **41**, R2483 (1990).
[13] C. Simenel, B. Avez, and C. Golabek, in Proceedings of the International Conference on Interfacing Structure and Reactions at the Centre of the Atom, Queenstown, 2008, edited by I. Thompson, arXiv:0904.2653 (unpublished).
[14] C. Golabek *et al.*, Int. J. Mod. Phys. E **17**, 2235 (2008).
[15] J. Tian, X. Wu, K. Zhao, Y. Zhang, and Z. Li, Phys. Rev. C **77**, 064603 (2008).
[16] P. A. M. Dirac, Proc. Cambridge Philos. Soc. **26**, 376 (1930).
[17] T. Skyrme, Philos. Mag. **1**, 1043 (1956).
[18] E. Chabanat, P. Bonche, P. Haensel, J. Meyer, and R. Schaeffer, Nucl. Phys. A **635**, 231 (1998).
[19] B. Avez, C. Simenel, and Ph. Chomaz, Phys. Rev. C **78**, 044318 (2008).
[20] Y. M. Engel *et al.*, Nucl. Phys. A **249**, 215 (1975).
[21] P. Bonche, S. Koonin, and J. W. Negele, Phys. Rev. C **13**, 1226 (1976).
[22] K.-H. Kim, T. Otsuka, and P. Bonche, J. Phys. G **23**, 1267 (1997).
[23] A. S. Umar and V. E. Oberacker, Phys. Rev. C **73**, 054607 (2006).
[24] J. A. Maruhn, P.-G. Reinhard, P. D. Stevenson, and M. R. Strayer, Phys. Rev. C **74**, 027601 (2006).
[25] C. Simenel, B. Avez, and D. Lacroix, arXiv:0806.2714.
[26] C. Simenel, Ph. Chomaz, and G. de France, Phys. Rev. Lett. **86**, 2971 (2001); Phys. Rev. Lett. **93**, 102701 (2004); Phys. Rev. C **76**, 024609 (2007).
[27] C. Simenel and B. Avez, Int. J. Mod. Phys. E **17**, 31 (2008).
[28] K. Washiyama and D. Lacroix, Phys. Rev. C **78**, 024610 (2008).
[29] K. Washiyama, D. Lacroix, and S. Ayik, Phys. Rev. C **79**, 024609 (2009).
[30] M. Schädel *et al.*, Phys. Rev. Lett. **41**, 469 (1978).
[31] M. Assié and D. Lacroix, Phys. Rev. Lett. **102**, 202501 (2009).
[32] D. Lacroix, S. Ayik, and Ph. Chomaz, Prog. Part. Nucl. Phys. **52**, 497 (2004).
[33] M. Tohyama and A. S. Umar, Phys. Rev. C **65**, 037601 (2002).
[34] X. Wu, J. A. Maruhn, and W. Greiner, J. Phys. G **10**, 645 (1984).